1 Abrupt climate change and millennial-scale cycles: an astronomical mechanism

Alison M. Kelsey

School of Earth and Environmental Sciences, The University of Queensland

Correspondence to: Alison Kelsey (alison.kelsey@uqconnect.edu.au)

Abstract. Contributing to the poor understanding of abrupt climate change is the lack of a known mechanism for a ~1470-yr quasi-periodicity, leading to debates as to its existence. This oscillation is associated with the controversial Bond cycle, which has been by some as stochastic resonance, and is a harmonic resonating with Heinrich, Dansgaard-Oeschger ice-rafting debris events, as well as millennial-scale ENSO events in the Pacific. Suggestions of a solar link to the Bond cycle were made but there is no known solar periodicity of this length. Here, statistically-significant results of a comparison between TSI reconstructions based on Antarctic ^{10}Be data and the modelled interaction of the solar and lunar cycles that produce a 1470-yr cycle are presented. These results confirm the cycle's existence, its astronomical mechanism, and the major lunar role in the timing of all these ice-rafting debris events. The associated data show that the occurrence of Bond events coincides with maximum gravitational forcing and peak TSI, both associated with minimum Sun-Earth distance that are influenced by both the perihelion and the Moon. These findings are consistent with previous suggestions by Bond and other researchers that amplified gravitational and solar forcing may be involved. The results also indicate that the Moon's gravitation influences patterns of cosmogenic isotopes at millennial time-scales.

1 Introduction

Although the mechanism of abrupt climate change is unknown, indicators exist, inferring that it may be astronomically-forced (Bond et al., 2001, Braun et al., 2005, Rahmstorf, 2003). Understanding this mechanism is an important step in understanding the physics of abrupt climate change. It has the capacity to inform our current understanding of Earth's cosmogenic nuclide record, which is important for radiometric dating in various scientific fields. Given that climate-change modelling relies on knowledge of the past to inform the future (Budyko, 1982), this astronomical mechanism is important because it influences total solar irradiance (TSI) and cosmogenic nuclides upon which climate reconstruction depends. An understanding of natural climate cycles is integral to understanding the nature and extent of anthropogenically-induced climate change and climate sensitivity.

Here, the arguments for and against the controversial Bond cycle are presented, along with relevant background astronomical and calendrical information, prior to presentation of modelling and results that reinforce the existence of an ~1470-yr quasi-periodicity. Variations in Sun-Earth, Sun-Moon distances are key to producing variations in total solar irradiance (TSI), solar insolation, and gravitational forcing that are associated with abrupt climate change at the millennial scale. Whilst various cycles at different time scales are produced by this interaction, of particular interest is the ~209 Suess de Vries cycle (SdV) and a hithero unexplained 133-yr cycle. This astronomical mechanism also explains why tidal and solar records are synchronised in the palaeoclimatic record (e.g., Bond et al., 1997) as the result of an external forcing mechanism. 'Teleconnections' between hemispheric records, as mentioned by Turney et al. (2004), can also be explained by this same mechanism for the same reasons, consistent with the Bipolar Seesaw theory (Broecker, 1998).

2 Background

A periodic or quasi-periodic characteristic in climate is suggestive of external forcing (Rahmstorf, 2003). The Milankovitch precessional cycle is itself a quasi-periodicity that results in a constantly changing relationship between the seasons and perihelion (Berger, 2009), the closest point in Earth's orbit to the Sun, over ~21±2 ky. The perihelion moves forward through the year over a cycle of ~110 ky (Lowrie, 2007), whilst the equinox moves in retrograde motion through the year over ~26 ky as the result of equinoctial precession. The Moon contributes two-thirds to the equinoctial precessional cycle and the Sun contributes one third through gravitational forcing (Lowrie, 2007). Based on a premise that precession causes abrupt climate change at higher temporal resolution than Milankovitch precession, the interaction of Earth's solar and lunar cycles was examined.

Millennial-scale, cyclical ice-rafted debris (IRD) events in the North Atlantic are associated with abrupt climate change, which is characterised by rapid warming then gradual cooling. These IRD events have been associated with the Dansgaard-Oeschger and Bond "cycles". Dansgaard-Oeschger oscillations in atmospheric temperature are found in the Greenland ^{18}O ice-core record of the glacial period, occurring at transitions from cold stadial to warm interstadial during the glacial period (Bond et al., 1997, Dansgaard et al., 1993, Schulz, 2002, Wolff et al., 2010) The Bond cycle was defined as a weaker and shorter climate signal permeating both the Holocene and glacial, with a mean periodicity of ~1470 yrs (Bond et al., 1999). Bond et al. (1999) identified this quasi-periodic oscillation to which Dansgaard-Oeschger and Heinrich events appeared to be tuned, meaning that the underlying Bond quasi-periodicity is a low amplitude signal that appears to be magnified at the times of Dansgaard-Oeschger and Heinrich events.

Heinrich events are massive discharges of IRD into the North Atlantic that occur at occur on a 11±1 ky periodicity (Bond et al., 1999, Heinrich, 1988, Summerhayes, 2015) and are therefore linked to the Milankovitch precessional cycle. Both Heinrich and Bond events showed clear associations with the modulation of the solar signal (Heinrich, 1988, Bond et al., 1999), the former as a precessional signal. Statistically-significant coherence between cosmogenic nuclides and IRD events with inferred solar frequencies of 500 yrs, 1 ky and 2 ky was established in relation to Bond events (Bond et al., 2001). However, the Bond cycle is controversial and has been dismissed by some as stochastic resonance (Ditlevsen et al., 2007), although the debate is clouded by a poor understanding of the physics of abrupt climate change (Ditlevsen and Ditlevsen, 2009, Banderas et al., 2015, Turney, 2008). Whilst stochastic resonance is a possibility for explaining this quasi-periodicity, it is conceivable that a combination of astronomical forcing factors could also produce this climate signal. Part of the problem in understanding the Dansgaard-Oeschger cycle is that "detection of periodicity depends on the age scale used", the asymmetry of events, and small sub-sampling of datasets (Wolff et al., 2010:2831). What has not been considered was a quasi-periodicity derived from multiple contributing astronomical periodicities.

The cause of the ~1470-yr pulse in ice-rafting debris (IRD) events in the North Atlantic is not known. Because no millennial-scale solar periodicities were apparent, an ocean-atmosphere link through solar forcing was suggested via a combination of periodicities (Bond et al., 2001, Braun et al., 2005, Schulz, 2002). Such suggestions were based on the coherence of the climate signal with cosmogenic nuclides. Turney et al. (2004) also demonstrated the existence of a ~1490-yr cycle in the tropical Pacific that was cross-correlated with the Dansgaard-Oeschger signal in the GISP2 ice-core record, where warm phases in the southern hemisphere were correlated with cold phases of Dansgaard-Oeschger events. Multiple records from around the world show a quasi-periodicity of this length, indicating the signal is global, e.g., (Clement and Peterson, 2008, Darby et al., 2012, van Buren, 2001).

80 Rahmstorf (2003) investigated the origin and stability of millennial-scale abrupt climate change cycles and Dansgaard-
81 Oeschger events. Rather than being a cycle, he concluded that (i) this cycle was paced by an external, regular 1470-yr orbital
82 cycle such as orbital or solar forcing, and (ii) realistically, errors due to triggering and dating would contribute significantly to
83 total deviations, whilst clock errors are much smaller than estimates. Braun et al. (2005) modelled the superposition of the
84 ~210-yr SdV cycle and the 86.5-yr Gleissberg cycle to emulate a ~1470-yr cycle of freshwater forcing of the thermohaline
85 current in the North Atlantic. In Braun et al.'s (2005) model, frequencies were inferred solar frequencies but no astronomical
86 mechanism was provided.
87
88 However, the modelled superposition of Earth's solar and lunar cycles has the capacity to produce oscillations at different
89 temporal scales, including millennial and centennial scales. (Figure 1). Modelling by Kelsey et al. (2015:4915) showed that
90 the Gleissberg cycle could result from the interaction of solar and lunar cycles (Figure 1). The concept of a specific
91 astronomical mechanism behind the ~1470-yr quasi-periodicity was introduced and was seen as a high-frequency expression
92 of the Milankovitch precessional cycle. The perihelion and the Moon were identified as variables because of their causal roles
93 in precession. This model showed cyclical interaction of the perihelion with the Metonic lunation (~209 yrs). The proxy used
94 in this model for the perihelion, with a value of 103.77 yrs is simply a precise and accurate measurement of the anomalistic
95 year based on Earth's rotation-revolution relative to the perihelion [Figure S1]. As such, this proxy's occurrence at 207.54 yrs
96 in conjunction with the Metonic New Moon is indicative of increased gravitational forcing, as well as suggestive of a
97 relationship with the sunspot cycle.
98
99
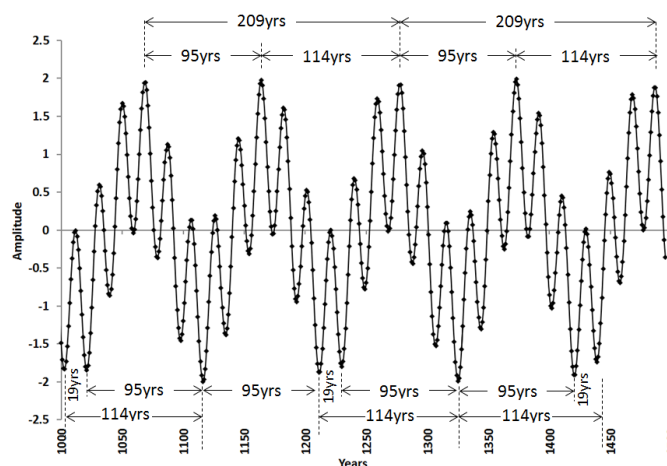
100 **Figure 1: Suess de Vries and Gleissberg cycles. The modelled superposition of solar and lunar cycles reproduces the Suess de Vries**
101 **(SdV) (209 yrs) and Gleissberg cycles (95 yrs)). This model captures the interaction of Earth's perihelion with the 19-yr Metonic**
102 **lunation: a time of maximum gravitational forcing.**
103
104 Throughout Earth's climatic record, 133-yr and ~208-yr periodicities are pervasive. The 133-yr cycle is found in various
105 climatic datasets, such as tropical Atlantic cyclones and water levels (Cohen and Sweetser, 1975, Yousef, 2000); fire and
106 drought cycles (Biagioni et al., 2015, Vázquez et al., 2015, Xue et al., 2008); and Arctic and Antarctic ice core chronologies
107 (Yiou et al., 1997). The SdV cycle, is an inferred solar cycle from the cosmogenic nuclide record (Hathaway, 2010). Because
108 the SdV cycle does not appear in the sunspot record, the inference is drawn because the SdV is a multiple of the longest known
109 solar cycle (Schwabe): an ~11.4-yr cyclical variability in solar luminosity (Hathaway, 2010). In association with the sunspot
110 cycle, the Metonic lunation is also a mathematical factor in the SdV (19 x 11 = 209). The Metonic cycle is a lunation that
111 occurs once every 19.0002 tropical years (O'Neil, 1975) and is used for synchronisation between solar and lunar calendars.

112   With a combination of periodicities theorised as producing the controversial Bond cycle and the existence of candidate
113   periodicities evidenced in palaeoclimatic data, research was undertaken to test an hypothesis of astronomical forcing
114   mechanism for the ~1470-yr cycle.

115   **2.1 Questioning the 1500-yr quasi-periodicity**

116   Whilst stochastic resonance is a possibility for explaining this quasi-periodicity, it is conceivable that a combination of
117   astronomical forcing factors could also produce this climate signal. What has not been considered was a quasi-periodicity
118   derived from multiple contributing periodicities. Part of the problem in understanding the Dansgaard-Oeschger cycle is that
119   "detection of periodicity depends on the age scale used", the asymmetry of events, and small sub-sampling of datasets (Wolff
120   et al., 2010:2831). Additionally, uncertainty associated with various ice core models have been troublesome.
121

122   Alley et al. (2001) suggested that the ~1500-yr peaks in the ^{18}O signatures from Greenland ice-cores could be potentially
123   explained by stochastic resonance within the climate system, triggered by random freshwater flux into the North Atlantic,
124   although stating that this did not constitute proof. Stochastic resonance produces a ripple effect through a system from a random
125   event, growing weaker with each periodic return. Alley et al. (2001) supported the existence of the quasi-periodicity and
126   believed that stochastic resonance model could be a contributor. They suggested that the stochastic resonance theory could be
127   tested later. In relation to the number and timing of Dansgaard-Oeschger events,
128

129   "asymmetry in Dansgaard-Oeschger oscillations …. causes the times of coolings to depend upon the threshold
130   to define a cooling, whereas times of warmings are less sensitive to the threshold chosen" (Alley et al., 2001:195).
131

132   Ditlevsen and Ditlevsen (2009) dismissed the ~1500-yr quasi-periodicity as random, noise-driven, and potentially stochastic
133   based on their redefinition of Dansgaard-Oeschger events. The redefinition process used by Ditlevsen et al. (2005) used
134   commonalities in the GRIP and NGRIP ice core records in an attempt to provide an objective definition (Ditlevsen et al., 2007,
135   Ditlevsen and Ditlevsen, 2009). Consequently, new events were classified and one declassified (DO9). In a later test using the
136   GISP2 record, the rejection of a strict periodicity could be achieved only by eliminating a Dansgaard-Oeschger event (DO9).
137   This DO9 event occurred at about 40 kya, which was at the edge of the period tested in these studies (11-42 kya) (Ditlevsen et
138   al., 2007). With DO9 removed, the 1470-yr cycle was then "indistinguishable" from a random event (Ditlevsen et al.,
139   2007:129). (Wolff et al., 2010) consider this matter to be unresolved.
140

141   A high band-pass filter was used to eliminate variations in the isotope record due to astronomical forcing at Milankovitch
142   scales (Ditlevsen et al., 2005, Ditlevsen et al., 2007). The low band-pass filter was selected on shared commonalities between
143   GRIP and NGRIP ice core records, which resulted in all signals of <30 yrs cyclicity being filtered out as background noise.
144   This process excluded signals generated by the Sun and Moon considered in this research. New thresholds in the isotope record
145   were also established to identify Dansgaard-Oeschger events: one high and one low. An upper threshold was established
146   through the use of stochastic resonance models that assume the signal is random and not externally forced (Ditlevsen et al.,
147   2005).
148

149   In their analysis of this quasi-periodicity from the filtered record, Ditlevsen et al. (2007) used three different model types
150   (exponential distribution, periodic, and stochastic resonance), with assumptions of randomness for the exponential model, and
151   a "perfect periodic signal" of 1470 yrs, for the periodic and stochastic resonance models. They then attempted to capture the
152   variability of the 1470±500-yr quasi-periodicity using a standard deviation of ±100 yrs. They concluded that the null hypothesis
153   of no periodicity could not be rejected, and that there was "no long-term memory in the climate system or unknown 1470-yr

154 periodic triggering of the climate shifts" (Ditlevsen et al., 2007:134). On one hand they state that statistical distribution of this
155 quasi-periodicity "implies" that the climate system has a simple no-memory process. Thereafter, this implication is specifically
156 stated as "fact" (Ditlevsen and Ditlevsen, 2009:446). Given the nature of the various ice-core records and chronologies, which
157 are complicated by chronometric uncertainties and disparities between various records, it is difficult to understand this
158 transition from implication to fact. These Ditlevsen models were not designed to deal with quasi-periodicities, using only
159 assumptions of randomness or perfect periodic beating.

160

161 Furthermore, the models used by Ditlevsen et al. (2007) have not considered the influence of some astronomical forcing factors
162 on the timing signals. An example of this is chronometric complications caused by precession, resulting from the inconstant
163 rate of the March equinox movement relative to the changing shape of Earth's elliptical orbit. This factor must influence the
164 length of the periodicity, which is exacerbated when the time-series is sub-sampled. Precession influences both the timing and
165 strength of the climate signal due to the changing relationship between Earth's seasonal year and changing orbital shape. When
166 considering astronomical cycles over very long periods, chronological precision is extremely important, especially because of
167 these precessional influences. Despite the use of a perfect periodicity in their exponential model, the "waiting time" between
168 Dansgaard-Oeschger events assumed by Ditlevsen et al. (2007) was 2800 yrs, which varies by 57.1 yrs to the definition
169 supplied. The stochastic resonance model is also flawed in this instance, resting on a "precise periodicity" and approximations
170 of "waiting time" (Ditlevsen et al., 2007).

171

172 Given the prerequisite of the precision assumed for dating Dansgaard-Oeschger events in their modelling experiment
173 (Ditlevsen et al., 2007), any arguments based on this premise are undermined by the cycle's quasi-periodic nature and the fact
174 that "all palaeoecological and palaeoclimatological data come with a degree of uncertainty" (Blaauw, 2012:38). The
175 combination of periodicities suggested as the cause of the Bond and Dansgaard-Oeschger cycles (Bond et al., 1997) is unlikely
176 to result in a periodicity of a precise length, particularly if multiple factors are involved. Ditlevsen et al. (2005) acknowledged
177 a similar point, citing Paillard and Labeyriet (1994) as "only simplified models with few degrees of freedom exhibit strict
178 cyclic behaviour". Clemens (2005) emphasises the importance of accurate chronologies, noticing that millennial-band
179 frequencies are sensitive to small changes in the modelled centennial-scale patterns on which they are based.

180

181 Other issues with the aforementioned Ditlevsen papers include the use of a monotonic function and assumptions about the
182 Gaussian form of dates based on strict periodicity (Ditlevsen et al., 2007). What has not been taken into account is the fact that
183 the radiocarbon calibration curve is not a monotonic function and the derived distribution of calendar dates for the data from
184 radiocarbon dating "is no longer Gaussian, nor is mathematically definable" (Bowman, 1990:46). For example, variations in
185 the radiocarbon curve caused by the 209-yr SdV cycle result in a radiocarbon date that can equate to more than one calendar
186 date (cf. Bowman, 1990). Calendar dates should be regarded as a range of equally likely dates, not as a central term with an
187 error margin (cf. Bowman, 1990, Dincauze, 2000).

188

189 To place the Ditlevsen dismissal of the 1500-yr quasi-periodicity as a real phenomenon in context, Alley et al. (2001:196) state
190 that "No finite data sequence ever uniquely defines the process that produced it." This is in keeping with the notions that the
191 use of empirically-derived models risk arguments of circularity being levelled against them (cf. Henshilwood and Marean,
192 2003, Popper, 1972). The testing and development of such models require a good understanding of the data in order to
193 compensate for problems associated with the use of statistics on non-linear and non-stationary geographic data, the nature of
194 which violates statistical assumptions (Longley, 2011, Mitchell, 1999, Schulz, 2002). If the cause of the quasi-periodicity is
195 not known or understood, this makes the job even more difficult. This is a problem acknowledged by Ditlevsen and Ditlevsen

196   (2009:446): "Dansgaard-Oeschger (DO) events of rapid climate shifts in the glacial climate observed in the Greenland ice

197   cores are still not well understood."

198

199   Referencing Ditlevsen et al. (2007) and Clemens (2005), Obrochta et al. (2012:25) dismiss the 1470-yr quasi-periodicity stating

200   that the signal is "absent from other Greenland ice cores". The Ditlevsen arguments have already been discussed. In contrast

201   to these claims that the 1470-yr cycle is absent from Greenland ice cores, Clemens (2005) reports (i) a bifurcation of the signal

202   into 1163-yr and 1613-yr peaks in the GRIP spectrum, and (ii) spectral peaks in GISP2 (tuned to the Hulu Cave record) of

203   1190, 1490, and 1667 years. Additionally, Clemens (2005) historical perspective of this cycle highlighted that it was evident

204   throughout the last 100 ky years in the GRIP SS09 model, and strong in the 20-40ky period in GISP2. These two chronologies

205   agree well where layers are counted, but differ significantly between 40-80 kya when "age models are based on independent

206   glaciological flow models" (Clemens, 2005:522).

207

208   Whereas the GISP2 chronology is layer counted to ~51 kya (Rahmstorf, 2003), based on visual stratigraphic layers, and

209   sometimes refined using laser scattering, oxygen isotope chronology, and electrical conductivity (Meese et al., 1997); GICC05

210   is based on NGRIP records between 10-42 kya, the SS09SEA model beyond 60 kya (after reducing the SS09SEA scale by 705

211   yrs at 60 kya) and annual layer counting (42-60 kya) (Svensson et al., 2006, Wolff et al., 2010). The NGRIP chronology is

212   based on the GRIP SS09SEA model (Svensson et al., 2006), which is an ice-flow model that factors in the $^{18}O:^{16}O$ relationship

213   (Svensson et al., 2008), and with which the GICC05 model agrees well (Wolff et al., 2010);this is not surprising given that

214   GICC05 is based on both models. However, whilst the 1470-yr quasi-periodicity is evident in a number of Greenland ice cores

215   over the past 120 ky (Rahmstorf, 2003), the GICC05 modelling alters the patterns of the Dansgaard-Oeschger cycle between

216   its tie-points (Ditlevsen et al., 2007). Whilst the 1470-yr cycles are best developed in MIS3 using the GISP2 Meese/Sowers

217   model (Bond et al., 1999), Obrochta et al. (2012) found that they were best developed during MIS4, which is based on the

218   SS09SEA glaciological model.

219

220   Apart from the aforementioned arguments raised by Obrochta et al. (2012) to dismiss the existence of a 1500-yr cycle, they

221   frequently reinforced their argument with the point that no solar cycle of that length exists. However, Bond et al. (2001) found

222   coherency of IRD events in various North Atlantic deep-sea cores with cosmogenic nuclide production, specifically ^{10}Be and

223   ^{14}C, and matched these events to other records from around the world during the Holocene, including (i) ^{18}O fluctuations in a

224   well-dated-stalagmite core from Oman, (ii) advances of Scandinavian glaciers linked to dendrochronological ^{14}C variations,

225   (iii) and evidence of abrupt climate change from other sources of atmospheric, lacustrine, and oceanic variations. Obrochta et

226   al. (2012) argued that the coherency was not at 1500 yrs, but at 500, 1000, and 2000 yrs, ignoring Clemens (2005) finding of

227   spectral peaks in GRIP and GISP records close to the 1500-yr mark and within the variability of this quasi-periodicity.

228

229   These conclusions by Obrochta et al. (2012) were based on a reinterpretation of the last 70ky North Atlantic record, using only

230   one of numerous deep-sea cores (Site 609) previously used by Bond et al. (1999, 2001). Previously, VM23-81 and Site 609

231   were extended by Bond further back in the glacial (beyond 26 kya) by transferring the GISP2 timescale to the foraminiferal

232   record in these cores using tie points, and interpolating between these records. Bond also used radiocarbon ages from VM23-

233   81 to construct a calendar age model for core SU90-24 that also enabled it to be extended further back into the glacial. In

234   contrast, Obrochta et al. (2012) updated the existing chronology on Site 609, using the latest marine calibration, extended it

235   back to 31 kya BP using additional radiocarbon dates, and superimposed NGRIP's GICC05 model further back in time. Whilst

236   Obrochta et al. (2012) imply that the whole of the GISP2 core is inferior to the NGRIP core due to thinning, this is not

237   accurately reported (cf. Svensson et al., 2006). There is generally a good match between GICC05 and GISP2 until 40kya

238   (Svensson et al., 2007), with layer thinning occurring during the early MIS3 in the GISP2 ice core (Svensson et al., 2006). Ice

239   layers are thin or absent during extreme cold (Svensson et al., 2006), which is also problematic for GICC05 (along with

240   resolution) during the glacial (Andersen et al., 2006).

241

242   Obrochta et al.'s (2012) conclusions fall short of effectively dismissing the 1500-yr quasi-periodicity. Firstly, their citation of

243   Clemens (2005) and Braun et al. (2005) was selective, and potential modification of solar forcing using heterodynes (Clemens,

244   2005) or combination tones (Braun *et al.*, 2005) was effectively overlooked in their conclusion. This oversight occurred despite

245   a statistically significant coherence between cosmogenic nuclide evidence with centennial- and millennial-scale IRD events

246   (Bond et al., 2001). Furthermore, their mathematical averaging argument that the 1500-yr cycle results from "1000 and 2000-

247   year forcing, similar to variability of inferred solar proxies" (Obrochta et al., 2012:32) provides no real solution as no known

248   solar cycle exists at either 1000-yrs or 2000-yr intervals, and the longest known solar cycle is ~11.4 mean years (Hathaway,

249   2010). The question still remains as to the cause of the apparent millennial-scale variability of proxies for solar variability (*viz*,

250   cosmogenic nuclides) and associated climate cycles. Finally, non-existence is not scientifically provable (cf. Popper, 1972).

3 Methods

252   Astronomical data were developed and graphed during exploratory data analysis, which mainly uses graphical techniques, to

253   gain insights into the interactive behaviour of the Sun, Moon and Earth. Additionally, a trigonometric model of the

254   superpositioned 133-yr and 207.5-yr cycles was implemented and adjusted for precession and sunspot activity. The 207.5-yr

255   cycle is associated with the anomalistic year and closely aligned to a 209-yr cycle associated with the Metonic lunation. These

256   models were compared to TSI reconstruction based on Antarctic ^{10}Be data (Bard et al., 2007).

3.1 Astronomical data

258   Astronomical data for the last 5500 yrs was generated using planetarium software. Data were collected at 19-yr intervals,

259   starting with the last Metonic lunation that occurred on the same day as Earth was at perihelion (4 January 2011). In this way,

260   the Moon serves as a proxy for the tropical year, and its movement can then be measured relative to the perihelion, to which

261   the anomalistic year is referenced. The point of osculation between the interacting variables is based on the Metonic lunation

262   at perihelion, which was a solar eclipse, when the Sun is at solar zenith. This point represents maximum annual gravitational

263   influences and solar irradiance, relative to any given starting longitude on Earth. It also provides a consistent baseline of

264   measurement of TSI, solar insolation, distance and gravitation throughout time, simultaneously chronologically anchoring it

265   to multiple methods of measuring time. Data recorded included solar and lunar declinations and longitudes, right ascension,

266   lunar nodal positions, and the obliquity of the ecliptic. Declinations are measured relative to the celestial equator and longitudes

267   relative to the ecliptic. These data were recorded using Gregorian dates and Universal Time. Earth-Sun and Earth-Moon

268   distances, and lunation type were also recorded as were variances of solar and lunar declinations. NOVA provides data back

269   to ~1221 BC while SkyChart III provides the earlier results.

3.2 Ice core data

271   The data used for comparison to the model are TSI reconstructions based on Antarctic ice-core data from the South Pole of

272   smoothed ^{10}Be record detailed in Bard et al. (2003-2007, Bard et al., 2007), as well as a superseded reconstruction by Yang et

273   al. (2000). These data span ~1200 yrs from 843 CE. The Bard TSI reconstruction used a 12-box numerical model to convert

274   ^{10}Be signals in ice-cores to a synthetic radiocarbon record (Bard et al., 2007). This reconstruction of TSI was found to strongly

275   correlate with the dendrochronologically-calibrated radiocarbon record (r=0.81), also showing no significant lag between the

276   ^{10}Be and radiocarbon records.

3.3 Model – trigonometric

278   The superpositioning of the 133-yr and 207.5-yr periodicities was modelled, using the formula:

$$f(t) \ = \ \sin((2\pi t) \, . \, 133^{-1}) \ + \ \sin((2\pi t) \, . \, P^{-1}) \tag{1}$$

279   where t=time elapsed (in years) since the start of the cycle and P=207.54 yrs as a measure of the anomalistic year. This model

280   captures the 133-yr cycle found in the astronomical data of fluctuations of Earth-Sun and Earth-Moon distance. The amplitude

281   of each contributing signal is assumed to be the same as both astronomical cycles are associated with variations in solar

282   irradiance based on changes in Earth-Sun distance. For S = 1365 W/m^2 where S (mean solar irradiance), which is the value

283   used by Bard et al.(2003-2007), the result for each value in the above equation was added to this mean TSI value in the

284   normalisation process, such that:

$$f(t) \ = \ (\sin((2\pi t) \, . \, 133^{-1}) \ + \ \sin((2\pi t) \, . \, P^{-1})) \ + \ S \ (W/m^2) \tag{2}$$

285

286   These models were chronologically-anchored at the concurrence of the Metonic lunation and the December solstice in 1183

287   BCE: a time of maximum gravitational forcing during a total solar eclipse [Figure S2] and the start of a new phase. The model

288   of the superimposed sinusoids was further normalised (feature-scaled) to the data being tested, e.g., where 1 unit of the model's

289   amplitude equals 0.7 W/m^2 (cf. Vieira et al., 2012). The value assigned to the amplitude during the normalisation process is

290   an estimate to cater for a number of factors, including annual variation in TSI during the year, such as orbital eccentricity

291   (±0.81 W/m) (Vieira et al., 2012); see also Tables S1 to S4. The model was then compared to Bard et al.'s (2007) TSI

292   reconstruction based on smoothed ^{10}Be record measured at South Pole. Statistical tests were performed (Pearson's X^2

293   goodness-of-fit; regression analysis).

294   3.4 Justification of TSI values used in model

295   The variation in TSI is not constant through time (cf. Feulner, 2011, Vieira et al., 2012). TSI varies due to changes in Earth-

296   Sun distance and sunspot activity, and is dependent upon time of year, and strength of and temporal position within the sunspot

297   cycle. Over long stretches of time, TSI levels in any particular season will vary due to precessional drift. Additionally,

298   reconstruction of TSI values prior to recorded observations are reliant on modelling and proxy data, such as cosmogenic

299   isotopes (Feulner, 2011, Vieira et al., 2012). One study identifies a difference of 0.2-0.7 W/m^2 at the time of solar minima

300   between the Maunder Minimum and 2008/2009 (Feulner, 2011). During the 3 previous solar cycles to 2012, TSI varied by

301   0.12%. Although the value for differences between sunspot minima and maxima is still debated, there is currently a consensus

302   that this value is ~0.12% (0.001) of total insolation, equivalent to ~1.6 W/m^2) (Friis-Christensen and Lassen, 1991, Kopp and

303   Lean, 2011, Vieira et al., 2011, Weng, 2005).

304   3.4.1 Adjustments for sunspot maxima and minima

305   For the model, TSI was increased by 0.12% during the Medieval Warm Period (high sunspot activity and auroral sightings)

306   and for relatively high sunspot activity during modern times (cf. Hathaway, 2010, Kopp and Lean, 2011, Vieira et al., 2011).

307   TSI was decreased by 0.05% and 0.1% respectively during the Maunder and Spörer Minimums based on an estimated 0.7

308   W/m^2 difference between the 2008 solar minimum and the Maunder Minimum (cf. Feulner, 2011).

309   3.5 Background to chronological measurement

310   Adjustments for precession are dependent upon how time is measured so some background is important in understanding the

311   adjustments made for precession (see below). The tropical, anomalistic, and sidereal years are all based on measurements of

312   Earth's rotation relative to different starting points, which respectively are the March equinox, the perihelion, and the fixed

313   star framework. Calendars vary in their attempt to measure the seasonal or tropical year, with the relevant ones to this

314   discussion being the Julian and Gregorian calendars. Earth's tropical (seasonal year) moves slowly backwards through the

315 calendar year, with the size of the differences due to the ability of the calendar year to adapt. The perihelion moves forward

316 through the tropical year.

317 Based on Earth's rotation [Tables 1 & 2], Figure 2 is a schematic showing the relationship of

318 the different year types relative to the others through a cycle of 2922 yrs. It can be seen that

319 the Gregorian calendar (G) closely mimics the tropical year (T) movement, whereas both the

320 Julian (J) and Anomalistic (A) years are in apparent opposite motion to the tropical and

321 Gregorian years. Thus AG = AT-GT; this relationship is numerically expressed in Table 2,

322 where as part of a cycle: 0.017136º = 0.0174369º-0.0003009º. Table 1 shows that the lengths

323 of the various year types in days, and the residual of a day based on the overshoot of the

324 rotation to the starting longitude in both days and hours. Table 2 shows the separation rates

325 between the different year/calendar types in minutes based on values in Table 1, and also as

326 parts of a day and hour and are based on the values in Table 1.
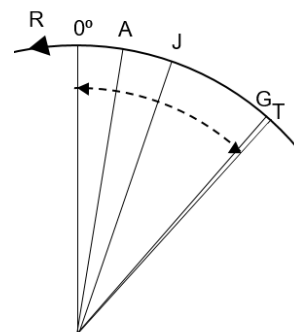
327 **Figure 2: Schematic of movement of different year/calendar types. The starting point is 0º of a cycle; A= anomalistic year; J=Julian**
328 **year; G=Gregorian year; T= tropical year. The direction of Earth's rotation (west to east) is indicated by arrow R. Thus, tropical**
329 **year is the shortest and anomalistic year is the longest, Schematic is an exaggeration of the actual movement although the proportions**
330 **between the different year lengths is preserved.**

331 **Table 1: Different year lengths measured in days and associated surplus of Earth's rotation (day, hrs).**

Year	Days	Day	Hrs
Anomalistic	365.2596	0.259636	6.231264
Sidereal	365.2564	0.25636	6.152641
Tropical	365.2422	0.242199	5.812778
Julian	365.25	0.25	6
Gregorian	365.2425	0.2425	5.82
Mean anomal/tropical	365.2059	0.205918	6.022021
Egyptian calendar	365	0	0

332

333

334 **Table 2: Relationships between year/calendar types, rotation values, and associated cycles. These rates are shown as portions of a**
335 **day, hour, and in minutes. The orbital scale cycle is based on the number of number of years in geographical return, which equals**
336 **1º of orbital cycle. The period produced based on the 1461-day Olympiad is calculated from the percentage of a rotation cycle (i.e.,**
337 **(1+0.0174369) x 1461=1486.48).**

Yr type relationship	Annual residual				Harmonic return (yrs)	Orbital scale cycle (yrs)	Length of cycle Julian (days, yrs)
	day (dec.)	% day	Hrs p.a. (dec)	Deg. Long.			
Anomalistic-tropical	0.0174	1.74369%	0.4185	6.28	57.35	20,645.87	1486.48
Sidereal-tropical	0.0142	1.41609%	0.3399	5.10	70.62	25,422.04	1481.69
Julian-tropical	0.0078	0.78009%	0.1872	2.81	128.19	46,148.52	1472.40
Julian-sidereal	0.0064	0.63600%	0.1526	2.29	157.23	56,603.42	1470.29
Julian-anomalistic	0.0096	0.96360%	0.2313	3.47	103.78	37,359.90	1475.08
Anomalistic-sidereal	0.0033	0.32760%	0.0786	1.18	305.25	109,891.45	1465.79
Gregorian-tropical	0.0003	0.03009%	0.0072	0.11	3323.36	1,196,410.77	1461.44
Gregorian-sidereal	0.0139	1.38600%	0.3326	4.99	72.15	25,973.95	1481.25
Gregorian-anomalistic	0.0171	1.71360%	0.4113	6.17	58.36	21,008.40	1486.04
Gregorian-Julian	0.0075	0.75000%	0.1800	2.70	133.33	48,000.00	1471.96

338

339 As the Earth rotates at 15º/hr, the number of degrees of separation per annum (geographic longitude) between each of the year

340 relationship types can be calculated [Table 2] and expressed as a proportion of any rotation cycle of 360º. For example, the

341 Gregorian and anomalistic year separate at a rate of 1.71% per annum; this rate is evidenced in the astronomical data developed

342   for this project, which gives the equation of the perihelion movement through the Gregorian calendar of y=0.0171x + 247.53,

343   where *x* is measured in years and *y* is longitude [Figure 3]. As can be seen [Table 2], the geographical return for the Gregorian-

344   anomalistic year occurs after 58.36 yrs. This value is very close to the actual values of the anomalistic and tropical year

345   separation (57.35 yrs) as the Gregorian calendar closely mimics the natural cycle. As the tropical and anomalistic year

346   separation produces the Milankovitch precessional cycle, over ~57.35 yrs the precessional separation is 1º producing a cycle

347   of ~20,646 yrs (~21,008 yrs Gregorian) [Table 2]. Similarly, the Gregorian-tropical relationship produces a cycle of ~3.3 ky,

348   which is the point at which the Gregorian calendar requires a further adjustment to realign with the tropical year.

349
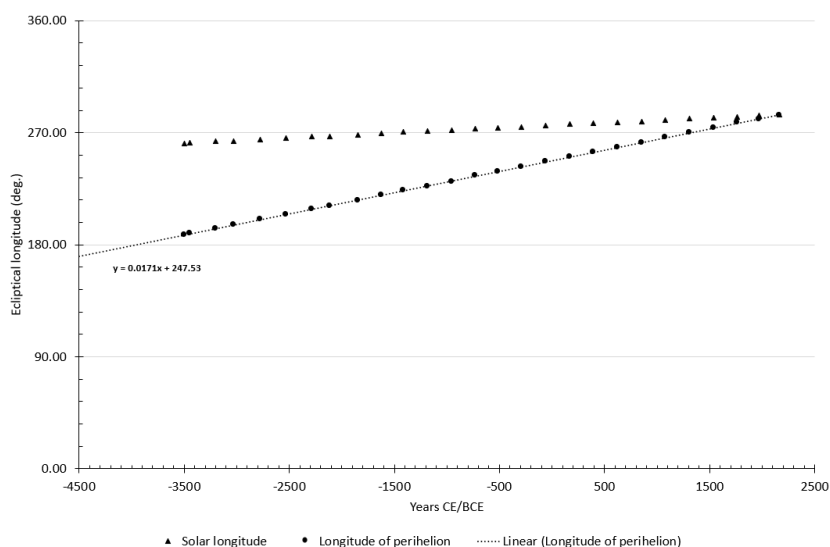
Figure 3: Longitudes of perihelion and Metonic lunation through time. This graph shows the relationship of the Metonic lunation and perihelion to the tropical year, derived from astronomical data. Negative values on the x-axis are BCE. Date of perihelion-December solstice conjunction at (270º) from this graph is 1308CE. The trend line equations are: y = 0.0171x + 247.53 (perihelion) and y = 0.0041x + 275.89 (Metonic lunation).

354

355   Whilst the Julian calendar is not equipped to keep pace with the tropical (seasonal) year the Gregorian calendar is well-adapted.

356   Whilst the difference between the Gregorian, tropical, and Julian years may not seem much, over large expanses of time this

357   error is cumulative. Clemens (2005) emphasises the importance of accurate chronologies, noting that millennial-band

358   frequencies are sensitive to small changes in the modelled centennial-scale patterns on which they are based.

359

360   Astronomical and climate data over long timespans and into the deep past are respectively recorded as Julian years, or uncal

361   BP or b2k (the latter of which are essentially Julian in nature). This is one of the reasons that these dates need to be calibrated

362   such as through absolutely dated tie-points or dendrochronology, the latter of which is a measurement of the seasonal year.

363   These chronometric systems, without calibration, do not account for either equinoctial or apsidal precession. Whilst the Julian

364   and tropical year Olympiads both contain ~1461 days (tropical 1460.969 days), the tropical year-Julian calendar produces an

365   ~1472-yr cycle [Table 2], effectively stretching the length of the cycle by ~11 yrs. Other Julian relationships are in this vicinity.

366

367   This stretching of the cycle is achieved in the same manner as the difference between the sidereal and solar days, where the

368   Earth has to rotate 4 minutes further to catch up to the solar position, (cf. O'Neil, 1975) whose apparent location has changed

369   due to Earth's movement along its orbital path. The relationship can be seen in Table 3, which shows that 1 day = 1º = 1 yr.

370   Table 3 shows that after 1461 yrs the vernal point of the spring equinox occurs approximately 11.4 days earlier (as 353 days

371   is ~11.4 days short of a full tropical year). This relationship is further confirmed at the annual scale where the cyclical

372 relationships of cycles embedded in cycles (hours, days, years) for the Gregorian-anomalistic year (0.0171) [Table 2] is the

373 same as the annual rate expressed in Figure 3 for the movement of the perihelion through the Gregorian year.

374

375 **Table 3: Lunar relationship with IRD events and relationship between days, years, and degrees. The difference between a full Earth**
376 **rotation and the tropical year is 0.24 days, which is a surplus of a full cycle. After an Olympiad (4 yrs), which is the basis of calendar**
377 **corrections, nearly an extra day has accumulated, which is also equal to about 1° ecliptical longitude. Values of particular interest**
378 **have been bold-faced for easy comparison. There is a cyclical interaction between the New Moon and any given starting point in the**
379 **tropical year.**

Yrs	Earth Rotation (°) Surplus	Cycle (°)	No. of cycles	Hrs accum	Additional time (days)	Added time (length of cycle) (Dec.)		Vernal point position relative to starting position		Diff between residual and full (days)	Lunation cycle
1	87.19	0.2422	0.00	5.81	0.2422	0.0007		0			
4	348.77	**0.9688**	0.00	23.25	**0.9688**	0.0027	days	0			
1461	127,387.51	353.8542	0.98	8,492.50	353.8542	**0.9688**	yrs	0	353.85	days	
1477.5	128,826.18	357.8505	0.99	8,588.41	357.8505	0.9798	yrs	0	357.85	days	7.39	1st qtr
2955	257,652.36	715.7010	1.99	17,176.82	715.7010	1.9595	yrs	1	350.46	days	14.78	Full Moon
4432.5	386,478.54	1073.5515	2.98	25,765.24	1073.5515	2.9393	yrs	2	343.0671	days	22.18	3rd qtr
5910	515,304.72	1431.4020	3.98	34,353.65	1431.4020	3.9190	yrs	3	335.6754	days	29.57	New Moon

380

3.6 Adjustments for precession

382 The intention of this exercise is to measure the movement of the perihelion relative to the tropical year, thereby capturing

383 maximum solar forcing relative to the tropical year. However, because the Milankovitch precessional cycle results from the

384 movement of the perihelion through the tropical year and because the astronomical data are recorded in Gregorian dates, the

385 separation rates between the tropical and anomalistic years and Gregorian dates are highly relevant to any adjustment made to

386 the models for precession. Adjustments to the models were therefore made for the precessional separation between the tropical

387 and anomalistic years relative to the Gregorian calendar.

388

389 The data already accounts for the movement of the Gregorian-anomalistic year relationship, so an adjustment needs to be made

390 for the differences between the tropical and Gregorian years [see Table 2]. Whilst the Bard et al. data and reconstruction begin

391 at 843 CE, the model presented here is chronologically-anchored at 1183 BCE and must be brought into phase with the Bard

392 data by adjusting for apsidal precession (of the perihelion), where 1183 BCE is cycle year 0. This time adjustment of the cycle

393 number for precession, t_p, is made by adjusting time elapsed (t) in Equation 2 such that:

394

$$t_p = 1.0003009t \qquad (3)$$

3.7 Statistical tests

396 Statistical tests were used to compare the model of superimposed astronomical cycles and the TSI reconstructions of [10]Be data

397 (Bard et al., 2003-2007). Non-stationary and non-linear data violates fundamental assumptions of inferential statistics, such as

398 those of independence (autocorrelation) and distribution and therefore presents problems for statistical analysis. However,

399 non-parametric tests, such as the Pearson's X^2 goodness-of-fit test, are suitable for analysing non-linear and non-stationary

400 data such as astronomical cycles and geographic data. The X^2 test, is a test against the null hypothesis of observed versus

401 expected or predicted values, which is one of no difference. Initially, the critical X^2 value (X^2_c) is determined using an identified

402 α value (probability) and the degrees of freedom (df). The generally accepted α value is 5% or $\alpha=0.05$, which was used here.

403   If the X^2 statistic is greater than the X^2_c, then the null hypothesis of "no difference" between the expected and observed values

404   is rejected. If the X^2 statistic is less than the X^2_c, the null hypothesis is accepted.

405

406   Despite the violations of statistical assumptions in analysing non-stationary and non-linear data, compensations can be made

407   if the nature of the data is understood (Schulz, 2002). In testing superimposed sinusoids of astronomically forced cycles against

408   sea-surface temperature data (both of which are non-linear and non-stationary), Imbrie (1985) calculated the Pearson's

409   correlation coefficient (r) to test the strength of the relationship between a model of superimposed sinusoids and the data. In

410   the following tests upon the predictive model of superimposed sinusoids of astronomical cycles and the TSI reconstructions

411   of [10]Be data, X^2 and r values were calculated at each stage of the model development. As with Imbrie (1985), the data and

412   model were assumed to be stationary and independent, *contra* to the intrinsic nature of the data.

413   **4 Results**

414   **4.1 Astronomical data**

415   Earth-Sun and Earth-Moon distances revealed patterns of 133-yr cyclicity [Figure S3] that is also found in solar declination

416   data (Kelsey et al., 2015) [Figures S4, S5], which is influenced by the lunar orbit as it moves between extreme southern and

417   northern declinations. Declinations are the positions of celestial bodies measured relative to the celestial equator. The vertical

418   alignment of lunar orbital plane also straightens a little each synodic month as it "faces the Sun" (Gutzwiller, 1998). The lunar

419   gravitational influence on the Earth's axis explains the 133-yr cycle found in solar declinations. Earth-Sun distances [Figure

420   S3] show a 133-yr cycle that flattens out as the perihelion and December solstice reach a conjunction around 1308 CE, attaining

421   a minimum distance as the perihelion and Metonic lunation form a conjunction in 2163 CE [Figures S3, S6]. Also evident in

422   Earth-Moon distances is a clear millennial-scale quasi-periodicity based on relative lunar perigee [Figure 4], when distance is

423   minimal and gravitational forcing maximal. These instances of lunar perigee occur close to Bond events (300-400, 1400, 2800,

424   4200 yrs ago) (cf. Bond et al., 1997).
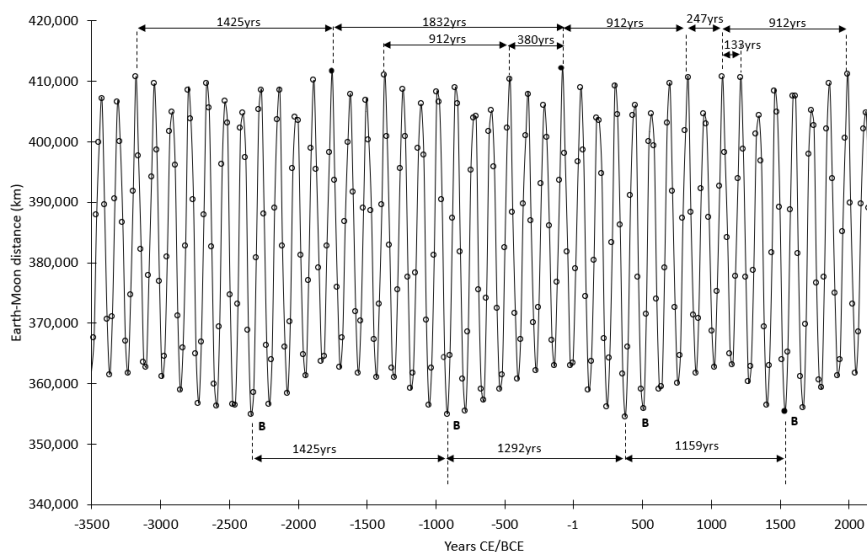
425

426   **Figure 4: Earth-Moon distances based on Metonic data. A basic oscillation of 133 yrs can be seen. Millennial-scale quasi-periodicities**
427   **can also be seen and are most pronounced at perigee. B marks the occurrence of a Bond IRD event at a time of reduced Sun-Earth**
428   **distance.**

429   These 133-yr cyclical patterns can be attributed to the dance between the Earth and Moon on their orbital paths. This figure

430   shows that at each New Moon, the Earth is periodically closer to the Sun than at Full Moon. As the Moon journeys around the

431   Earth, and the Earth around the Sun, their paths create sinusoidal patterns around their common barycentre. Naturally, when

432   the New Moon occurs close to perihelion the gravitational forces are stronger and distances smaller. The physical data show

433   that during the 133-yr cycle, minimum distances between Earth and Moon correspond with minimum distances between Earth

434   and Sun; they also share the timing of maximum distances. These distances influence both gravitational force and solar

435   irradiance levels.

436   **4.2 Modelling and statistical testing**
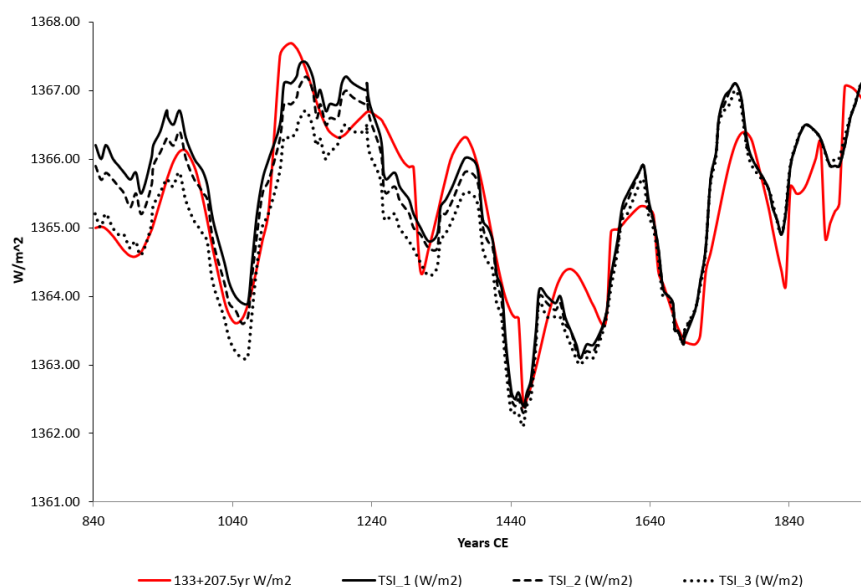
438   **Figure 5: The chronologically-anchored, normalised model adjusted for both sunspot minima and maxima and precession compared**
439   **to TSI reconstructions. Each of the TSI reconstructions is shown as indicated in the legend. TSI_1 is the original Bard reconstruction**
440   **(Bard et al., 2007), uncorrected for geomagnetic modulation; TSI_2 is corrected for geomagnetic modulation, with agreement**
441   **between Bard et al., Korte and Constable (2005), and Gubbins et al. (2006); TSI_3 is corrected for geomagnetic modulation based**
442   **on the superseded record of Yang et al. (2000). The black solid line is the model.**

443

444   The model of the superimposed 133-yr and 207.5-yr periodicities produced a cycle of 1470 tropical years (1459 Julian years)

445   [Figures 5, S7]. The model bears a strong visual resemblance to the TSI reconstructions based on Antarctic ^{10}Be; X^2 and

446   regression analysis serve to statistically quantify this relationship. The normalised, chronologically-anchored model, adjusted

447   for both precession and sunspot activity, shows a strong positive correlation [Figure S8] compared to the TSI reconstructions

448   from Antarctic ice core data (Bard et al., 2007). The results of the statistical tests are shown in Table 4. The X^2 results between

449   each of the reconstructions (TSI_1, TSI_2, TSI_3) were the same at $X^2=0.04$ well below the critical value ($X^2_c = 168.61$,

450   df=140 and $\alpha=0.05$). Therefore, the null hypothesis of no difference between the model and each of the reconstructions cannot

451   be rejected. There is no difference between the model and the TSI reconstructions.

452

453

454

455   **Table 4: Statistical results of X^2, r values. Variance (r^2), and significance (p) for precession and sunspot-adjusted**
456   **model.**

Stat test/period	TSI_1			TSI_2			TSI_3		
X^2	0.04			0.04			0.05		
Correlation/variance/significance	r	r^2	p	r	r^2	p	r	r^2	p
(entire period)	0.88	0.78	0.00	0.88	0.78	0.00	0.86	0.74	0.00
843CE-1481CE	0.88	0.78	0.00	0.89	0.80	0.00	0.92	0.84	0.00
1481CE-1829CE	0.87	0.76	0.00	0.86	0.75	0.00	0.86	0.73	0.00
1829CE-1961CE	0.85	0.72	0.00	0.85	0.72	0.00	0.86	0.74	0.00

457

458   For the full range of the model, TSI_1, TSI_2, and TSI_3 scored similarly for correlation (r=0.88 and r=0.86). These r values
459   show a strong positive correlation similar to the best results achieved by the TSI reconstructions detailed in Bard et al. (Bard
460   et al., 2007) compared to the dendrochronologically calibrated radiocarbon record (r=0.81). All results are statistically
461   significant (p<0.05). This result indicates that ~78% of the variation in TSI can be explained through the interaction of the
462   superpositioning of the 133-yr and 207.5 year solar and lunar cycles.

463   **5 Discussion**

464   A 1470-yr cycle was produced by the interaction of the 133-yr cycle of reduced Earth-Sun and Earth-Moon distances with the
465   perihelion (207.5-yr), which is closely aligned to the sunspot cycle, Metonic lunation, and SdV cycle. Modelling of the 133-
466   yr cycle interaction with the lunar-linked 209-yr cycle similarly produced a 1474-yr cycle (1463 Julian years) [Figure S9].
467   Statistical results from the superpositioning of the 133-yr and 207.5-yr cycles confirm the involvement of solar forcing at
468   ~1470 yrs, and also identify lunar forcing as a contributor through its effects on Earth-Sun and Earth-Moon distances.

469

470   Whilst sunspots and the solar wind modulate cosmic ray flux, evidenced in Earth's cosmogenic nuclide record, it is now
471   evident lunar gravitational forcing also shapes patterns of cosmogenic nuclides in the climate record at the millennial scale.
472   Such results are important to radiochronology as the amplitude and shape of the climate signal are influenced by chronological
473   models. For example, the Cariaco core (ODP1002) had an estimated calendar chronology based on correlation of visually-
474   identified stratigraphy with GISP2 ^{18}O record (Chiu et al., 2007). The application of various other Greenland ice-core
475   chronologies to this core altered the trends and amplitudes of the ^{14}C record.

476

477   For the SdV cycle (~208 yrs) that is found in the radiocarbon record, there is an inferred association with the perihelion
478   movement (207.5 yrs), Metonic lunation cycle (209 yrs), and sunspot cycle (~206 yrs). A 209-yr cycle is also found in lunar
479   declination data (Kelsey et al., 2015), which forms a sinusoidal pattern, consisting of four phases of 209 to 228 yrs [Figure
480   S10], with a cycle of 893-912 yrs. All these factors are influenced by distance relationships, consequently impacting on both
481   gravitation and TSI. Just as Earth's solar declination is affected by gravitation, so too is lunar declination. The 228-yr harmonic
482   was previously identified in radiocarbon data as a "mysterious" companion signal to the SdV signal (Damon and Peristykh,
483   2004:243) is also a phase length in the lunar declination data.

484

485   Reinforcing these radiocarbon associations is the coincidence of reduced variability in the solar declination cycle during the
486   second millennium BCE [Figure S4], concurrent with reduced variability of the SdV cycle in radiocarbon data (cf. Stuiver et
487   al., 1998). This reduction in both the solar declination and radiocarbon signals can be explained by the occurrence of the
488   Metonic lunation at the December solstice during this same period. Lunar declination is constrained by the ecliptic (the lunar
489   orbital plane is inclined at ~5° to the ecliptic). Because the solstices are the maximum southern and northern declinations, the

490   extremes of lunar declination are constrained by the turning points in solar declination. Similarly other associations between

491   frequencies found in palaeoclimatic data and astronomical features are also evident (Table S5).

492

493   The Gregorian and Julian calendars are based on the synthesisation of solar and lunar cycles. Just as combined solar and lunar

494   gravitational forcing produce the Milankovitch precessional cycle (~21±2 ky), so too is the ~1470-yr cycle, which is found in

495   records globally. The ~1470-yr 'cycle' can thus be seen as a high-frequency expression of the Milankovitch precessional

496   cycle. Thus millennial-scale ENSO events and North Atlantic ice-rafted debris (IRD) events can be seen as symptomatic of

497   this forcing, with variations based on physical geography. Such geographical variations also have the capacity to incorporate

498   the bipolar seesaw effect (cf. Broecker, 2003) and explain teleconnections linking northern and southern hemispheres (cf.

499   Turney et al., 2004). Effectively, the interaction between TSI, solar and lunar gravitational forces trigger responses in Earth's

500   oceans and atmospheres, such as the thermohaline current and ENSO's atmospheric transport of heat and moisture (Broecker,

501   2003).

502

503   The mean value for the Bond (1999) cycle during the Holocene and Glacial was given as 1469±514 yrs; for the Holocene as

504   1374±502 yrs; for the Glacial as 1476±585 yrs. Whilst the Bond cycle is a quasi-periodicity, underlying both Heinrich and

505   Dansgaard-Oeschger events, the individual contributions of the Sun and Moon as well as their interactions have the capacity

506   to account for variations in the length ~1470-yr quasi-periodicity. The strength of the solar signal (through the perihelion and

507   anomalistic year) varies due to a number of factors, including position of the perihelion relative to the seasonal year, the

508   precision of cyclical interaction between Earth, Sun, and Moon, as well as the interaction of the 133-yr cycle of variations in

509   distance with the perihelion.

510

511   Importantly, these IRD events and abrupt warming can also be seen to be linked directly to the lunation cycle [Table 3], as

512   days short of a full year (cyclical return). Effectively this means that the vernal point of the spring equinox has moved

513   backwards through the year relative to the calendar, fixed stars, and perihelion due to equinoctial precession. Gravitational

514   forcing is strongest at the New Moon, which occurs at ~29.53-day intervals, which cyclically occurs at 5910 yrs (the same

515   oscillation as Heinrich events) (cf. Mayewski et al., 1997). This means that after 5910 yrs, the vernal equinox has moved

516   retrograde by one synodic month. Next in strength is the Full Moon, occurring ~14.75 days later which is linked to the

517   Dansgaard-Oeschger oscillation at 2955 yrs. The First and Third Quarter lunar phases are next in strength and are clearly are

518   associated with the Bond cycle at ~1478 yrs. At times of solar and lunar eclipses, these events are magnified by increased

519   gravitational forcing. Essentially, the Bond cycle frequency, which underpins Dansgaard-Oeschger and Heinrich oscillations

520   cycle, is linked with the rhythmic phases of the Moon. As the New and Full Moons amplify this signal, so are Heinrich and

521   Dansgaard-Oeschger events amplifications of the Bond signal. These events would be further amplified at half the precessional

522   cycle as the New Moon come into contact with the perihelion where gravitational forcing is at a maximum.

523   **6 Conclusion**

524   Here it has been demonstrated that two cycles (133-yr and 207.5-yr), found in astronomical data (with counterparts in climate

525   cycles), together produce a ~1470-yr cycle. The astronomical mechanism for this forcing is comprised of fluctuations in Earth-

526   Sun and Earth-Moon distances that affect gravity, insolation, and TSI. A comparison between TSI reconstructions (Bard et

527   al., 2007) and the model (based on astronomical data) shows a statistically-significant, strong, positive correlation (r=0.88,

528   p=0); and that there is no difference between this model and previous TSI reconstruction based on ^{10}Be from the South Pole

529   (X^2=0.04; X^2_c = 168.61, df=140 and α=0.05). These results provide a new and important understanding of the physics of

530   climate change and radiochronological dating used by a variety of sciences.

531

532 This 1470-yr frequency is closely linked with Earth-Sun-Moon interaction, and offers a mechanical explanation for abrupt

533 climate change where previously none existed. The 1470-yr cycle is associated with the lunation cycle at multiple time scales.

534 The timing of these lunations at millennial scales with Heinrich, Dansgaard-Oeschger, and Bond events in the North Atlantic

535 reinforces its identity as a high-frequency expression of the Milankovitch precessional cycle; and fortifies its role in producing

536 abrupt climate change. This evidence negates previous suggestions that the ~1470-yr cycle is non-existent (Ditlevsen et al.,

537 2007), results from mathematical averaging (Obrochta et al., 2012), or that it may simply be a result of stochastic resonance

538 within Earth's climate system (Alley et al., 2001).

539 **Acknowledgements**

540 I thank the School of Earth and Environmental Sciences at the University of Queensland for research funding. I would also

541 like to thank Prof. Fred Menk, Prof. Patrick Moss, Prof. Peter Kershaw for their advice. There are no real or perceived conflicts

542 for the author.

543 **Author contribution:** 100%

544 **Competing interests:** None

545 **Code/Data availability:** Data is available at https://doi.org/10.14264/uql.2019.962

546 **Supplementary information** is available for this paper.

547 **References cited**

548 ALLEY, R. B., ANANDAKRISHNAN, S. & JUNG, P. 2001. Stochastic resonance in the North Atlantic.
549 *Paleoceanography,* 16**,** 190-198.
550 ANDERSEN, K. K., SVENSSON, A., JOHNSEN, S. J., RASMUSSEN, S. O., BIGLER, M., RÖTHLISBERGER, R., RUTH, U.,
551 SIGGAARD-ANDERSEN, M.-L., PEDER STEFFENSEN, J., DAHL-JENSEN, D., VINTHER, B. M. & CLAUSEN, H. B.
552 2006. The Greenland Ice Core Chronology 2005, 15–42 ka. Part 1: constructing the time scale. *Quaternary*
553 *Sci. Rev.,* 25**,** 3246-3257.
554 BANDERAS, R., ALVAREZ-SOLAS, J., ROBINSON, A. & MONTOYA, M. 2015. An interhemispheric mechanism for
555 glacial abrupt climate change. *Clim. Dynam.,* 44**,** 2897-2908.
556 BARD, E., RAISBECK, G., YIOU, F. & J., J. 2003-2007. Reconstructed Solar Irradiance Data. *In:* BARD, E., RAISBECK,
557 G., YIOU, F. & J., J. (eds.). IGBP PAGES/World Data Center for Paleoclimatology, NOAA/NGDC
558 Paleoclimatology Program, Boulder CO, USA.
559 BARD, E., RAISBECK, G. M., YIOU, F. & JOUZEL, J. 2007. Comment on "Solar activity during the last 1000 yr inferred
560 from radionuclide records" by Muscheler et al. (2007). *Quaternary Sci. Rev.,* 26**,** 2301-2304.
561 BERGER, A. 2009. Astronomical Theory of Climate Change. *In:* GORNITZ, V. (ed.) *Encyclopedia of Paleoclimatology*
562 *and Ancient Environments.* Dordrecht: Springer Netherlands.
563 BIAGIONI, S., KRASHEVSKA, V., ACHNOPHA, Y., SAAD, A., SABIHAM, S. & BEHLING, H. 2015. 8000 years of
564 vegetation dynamics and environmental changes of a unique inland peat ecosystem of the Jambi Province
565 in Central Sumatra, Indonesia. *Palaeogeogr. Palaeoecol.,* 440**,** 813-829.
566 BLAAUW, M. 2012. Out of tune: the dangers of aligning proxy archives. *Quaternary Sci. Rev.,* 36**,** 38-49.

567 BOND, G., KROMER, B., BEER, J., MUSCHELER, R., EVANS, M. N., SHOWERS, W., HOFFMANN, S., LOTTI-BOND, R.,
568   HAJDAS, I. & BONANI, G. 2001. Persistent solar influence on North Atlantic climated during the Holocene.
569   *Science,* 294, 2130-2136.
570 BOND, G., SHOWERS, W., CHESEBY, M., LOTTI, R., ALMASI, P., DEMENOCAL, P., PRIORE, P., CULLEN, H., HAJDAS,
571   I. & BONANI, G. 1997. A pervasive millennial-scale cycle in North Atlantic Holocene and Glacial climates.
572   *Science,* 278, 1257-1266.
573 BOND, G. C., SHOWERS, W., ELLIOT, M., EVANS, M., LOTTI, R., HAJDAS, I., BONANI, G. & JOHNSON, S. 1999. The
574   North Atlantic's 1-2 Kyr Climate Rhythm: Relation to Heinrich Events, Dansgaard/Oeschger Cycles and the
575   Little Ice Age. *Mechanisms of Global Climate Change at Millennial Time Scales.* American Geophysical
576   Union.
577 BOWMAN, S. 1990. *Interpreting the Past: Radiocarbon Dating,* Berkeley, University of California Press.
578 BRAUN, H., CHRISTL, M., RAHMSTORF, S., GANOPOLSKI, A., MANGINI, A., KUBATZKI, C., ROTH, K. & KROMER, B.
579   2005. Possible solar origin of the 1,470-year glacial climate cycle demonstrated in a coupled model.
580   *Nature,* 438, 208-211.
581 BROECKER, W. S. 1998. Paleocean circulation during the Last Deglaciation: A bipolar seesaw? *Paleoceanography,*
582   13, 119-121.
583 BROECKER, W. S. 2003. Does the trigger for abrupt climate change reside in the ocean or in the atmosphere?
584   *Science,* 300, 1519-1522.
585 BUDYKO, M. I. 1982. *The Earth's Climate; Past and Future,* New York, Academic Press.
586 CHIU, T.-C., FAIRBANKS, R. G., CAO, L. & MORTLOCK, R. A. 2007. Analysis of the atmospheric 14C record spanning
587   the past 50,000 years derived from high-precision 230Th/234U/238U, 231Pa/235U and 14C dates on
588   fossil corals. *Quaternary Sci. Rev.,* 26, 18-36.
589 CLEMENS, S. C. 2005. Millennial-band climate spectrum resolved and linked to centennial-scale solar cycles.
590   *Quaternary Sci. Rev.,* 24, 521-531.
591 CLEMENT, A. C. & PETERSON, L. C. 2008. Mechanisms of abrupt climate change of the last glacial period. *Rev.
592   Geophys.,* 46, RG4002.
593 COHEN, T. J. & SWEETSER, E. I. 1975. The /`spectra/' of the solar cycle and of data for Atlantic tropical cyclones.
594   *Nature,* 256, 295-296.
595 DAMON, P. E. & PERISTYKH, A. N. 2004. Solar and Climatic Implications of the Centennial and Millennial
596   Periodicities in Atmospheric Δ14C Variations. *Solar Variability and Its Effects on Climate.* American
597   Geophysical Union.
598 DANSGAARD, W., JOHNSEN, S. J., CLAUSEN, H. B., DAHL-JENSEN, D., GUNDESTRUP, N. S., HAMMER, C. U.,
599   HVIDBERG, C. S., STEFFENSEN, J. P., SVEINBJORNSDOTTIR, A. E., JOUZEL, J. & BOND, G. 1993. Evidence for
600   general instability of past climate from a 250-kyr ice-core record. *Nature,* 364, 218-220.
601 DARBY, D. A., ORTIZ, J. D., GROSCH, C. E. & LUND, S. P. 2012. 1,500-year cycle in the Arctic Oscillation identified
602   in Holocene Arctic sea-ice drift. *Nature Geoscience,* 5, 897-900.
603 DINCAUZE, D. F. 2000. *Environmental Archaeology: Principles and Practice,* Cambridge, Cambridge University
604   Press.
605 DITLEVSEN, P. D., ANDERSEN, K. K. & SVENSSON, A. 2007. The DO-climate events are probably noise induced:
606   statistical investigation of the claimed 1470 years cycle. *Clim. Past.,* 3, 129-134.
607 DITLEVSEN, P. D. & DITLEVSEN, O. D. 2009. On the stochastic nature of the rapid climate shifts during the last Ice
608   Age. *J. Climate,* 22, 446-457.
609 DITLEVSEN, P. D., KRISTENSEN, M. S. & ANDERSEN, K. K. 2005. The recurrence time of Dansgaard-Oeschger events
610   and limits on the possible periodic component. *J. Climate,* 18, 2594-2603.
611 FEULNER, G. 2011. Are the most recent estimates for Maunder Minimum solar irradiance in agreement with
612   temperature reconstructions? *Geophys. Res. Lett.,* 38.
613 FRIIS-CHRISTENSEN, E. & LASSEN, K. 1991. Length of the solar cycle: an indicator of solar activity closely associated
614   with climate. *Science,* 254, 698-700.
615 GUBBINS, D., JONES, A. L. & FINLAY, C. C. 2006. Fall in Earth's magnetic field is erratic. *Science,* 312, 900-902.
616 GUTZWILLER, M. C. 1998. Moon-Earth-Sun: the oldest three-body problem. *Rev. Mod. Phys.,* 70, 589-639.
617 HATHAWAY, D. H. 2010. The Solar Cycle. *Living Rev. Sol. Phys.,* 7, 1-65.
618 HEINRICH, H. 1988. Origin and consequences of cyclic ice rafting in the Northeast Atlantic Ocean during the past
619   130,000 years. *Quaternary Res.,* 29, 142-152.
620 HENSHILWOOD, CHRISTOPHER S. & MAREAN, CURTIS W. 2003. The origin of modern human behavior: critique of
621   the models and their test implications. *Curr. Anthropol.,* 44, 627-651.

622 IMBRIE, J. 1985. A theoretical framework for the Pleistocene ice ages: William Smith Lecture. *J. Geol. Soc. London,*
623   142, **417-432.**
624 KELSEY, A. M., MENK, F. W. & MOSS, P. T. 2015. An astronomical correspondence to the 1470 year cycle of abrupt
625   climate change. *Clim. Past. Discussions,* 2015, **4895-4915.**
626 KOPP, G. & LEAN, J. L. 2011. A new, lower value of total solar irradiance: Evidence and climate significance.
627   *Geophys. Res. Lett.* [Online], 38. [Accessed December 7, 2014].
628 KORTE, M. & CONSTABLE, C. G. 2005. Continuous geomagnetic field models for the past 7 millennia: 2. CALS7K.
629   *Geochemistry, Geophysics, Geosystems* [Online], 6. Available: http://dx.doi.org/10.1029/2004GC000801
630   [Accessed November 30, 2015].
631 LONGLEY, P. 2011. *Geographic information systems & science,* Hoboken, NJ, Wiley.
632 LOWRIE, W. 2007. *Fundamentals of Geophysics,* Cambridge, Cambridge University Press.
633 MAYEWSKI, P. A., MEEKER, L. D., TWICKLER, M. S., WHITLOW, S., YANG, Q., LYONS, W. B. & PRENTICE, M. 1997.
634   Major features and forcing of high-latitude northern hemisphere atmospheric circulation using a 110,000-
635   year-long glaciochemical series. *J. Geophys. Res-Oceans,* 102, **26345-26366.**
636 MEESE, D. A., GOW, A. J., ALLEY, R. B., ZIELINSKI, G. A., GROOTES, P. M., RAM, M., TAYLOR, K. C., MAYEWSKI, P.
637   A. & BOLZAN, J. F. 1997. The Greenland Ice Sheet Project 2 depth-age scale: methods and results. *J.
638   Geophys. Res-Oceans,* 102, **26411-26423.**
639 MITCHELL, A. 1999. *The ESRI guide to GIS analysis,* Redlands, Calif, ESRI Press.
640 O'NEIL, W. M. 1975. *Time and the Calendars,* Sydney, Sydney University Press.
641 OBROCHTA, S. P., MIYAHARA, H., YOKOYAMA, Y. & CROWLEY, T. J. 2012. A re-examination of evidence for the
642   North Atlantic "1500-year cycle" at Site 609. *Quaternary Sci. Rev.,* 55, **23.**
643 PAILLARD, D. & LABEYRIET, L. 1994. Role of the thermohaline circulation in the abrupt warming after Heinrich
644   events. *Nature,* 372, **162-164.**
645 POPPER, K. S. 1972. *Objective Knowledge: An Evolutionary Approach,* Oxford, Clarendon Press.
646 RAHMSTORF, S. 2003. Timing of abrupt climate change: A precise clock. *Geophys. Res. Lett.* [Online], 30.
647 SCHULZ, M. 2002. On the 1470-year pacing of Dansgaard-Oeschger warm events. *Paleoceanography,* 17, **1014.**
648 STUIVER, M., REIMER, J., BARD, E., WARREN BECK, J., BURR, G., HUGHEN, K., KROMER, B., MCCORMAC, G., VAN
649   DER PLICHT, J. & SPURK, M. 1998. Intcal98 radiocarbon age calibration, 24,000-0 cal BP. *Radiocarbon,* 40,
650   **1041-1083.**
651 SUMMERHAYES, C. P. 2015. Earth's Climate Evolution. http://onlinelibrary.wiley.com: Wiley Online Library.
652 SVENSSON, A., ANDERSEN, K. K., BIGLER, M., CLAUSEN, H., DAHL-JENSEN, D., JOHNSEN, S., RASMUSSEN, S. O.,
653   RÖTHLISBERGER, R., STEFFENSEN, J. P. & VINTHER, B. 2007. A new 60,000 year Greenland stratigraphic
654   ice core chronology. *4th EGU General Assembly.* Vienna, Austria.

655 SVENSSON, A., ANDERSEN, K. K., BIGLER, M., CLAUSEN, H. B., DAHL-JENSEN, D., DAVIES, S. M., JOHNSEN, S. J.,
656   MUSCHELER, R., PARRENIN, F., RASMUSSEN, S. O., RÖTHLISBERGER, R., SEIERSTAD, I., STEFFENSEN, J. P.,
657   VINTHER, B. M., NATURVETENSKAP, KVARTÄRGEOLOGI, SCIENCE, GEOCENTRUM, II, DEPARTMENT OF, G.,
658   QUATERNARY, S., LUNDS, U., GEOCENTRE, II, GEOLOGISKA, I., LUND, U., BIOLOGISK-GEOVETENSKAPLIGA,
659   V., SECTION OF, B. & EARTH, S. 2008. A 60,000 year Greenland stratigraphic ice core chronology. *Clim.
660   Past.,* 4, **47-57.**
661 SVENSSON, A., ANDERSEN, K. K., BIGLER, M., CLAUSEN, H. B., DAHL-JENSEN, D., DAVIES, S. M., JOHNSEN, S. J.,
662   MUSCHELER, R., RASMUSSEN, S. O., RÖTHLISBERGER, R., PEDER STEFFENSEN, J. & VINTHER, B. M. 2006.
663   The Greenland Ice Core Chronology 2005, 15–42 ka. Part 2: comparison to other records. *Quaternary Sci.
664   Rev.,* 25, **3258-3267.**
665 TURNEY, C. 2008. *Ice, Mud and Blood: Lessons from Climates Past,* Basingstoke, Palgrave Macmillan.
666 TURNEY, C. S. M., KERSHAW, A. P., CLEMENS, S. C., BRANCH, N., MOSS, P. T. & KEITH FIFIELD, L. 2004. Millennial
667   and orbital variations of El Nino/Southern Oscillation and high-latitude climate in the last glacial period.
668   *Nature,* 428, **306-310.**
669 VAN BUREN, M. 2001. The archaeology of El Niño events and other "natural" disasters. *J. Archaeol. Meth. Th.,* 8,
670   **129-149.**
671 VÁZQUEZ, A., CLIMENT, J. M., CASAIS, L. & QUINTANA, J. R. 2015. Current and future estimates for the fire
672   frequency and the fire rotation period in the main woodland types of peninsular Spain: a case-study
673   approach. *For. Syst.,* 24, **e031-e031.**
674 VIEIRA, L. E. A., NORTON, A., DUDOK DE WIT, T., KRETZSCHMAR, M., SCHMIDT, G. A. & CHEUNG, M. C. M. 2012.
675   How the inclination of Earth's orbit affects incoming solar irradiance. *Geophys. Res. Lett.* [Online], 39.

676   VIEIRA, L. E. A., SOLANKI, S. K., KRIVOVA, N. A. & USOSKIN, I. 2011. Evolution of the solar irradiance during the
677   Holocene. *Astron. Astrophys.* [Online], 531. [Accessed May 3, 2014].
678   WENG, H. 2005. The influence of the 11yr solar cycle on the interannual–centennial climate variability. *J. Atmos.*
679   *Sol-Terr. Phy.,* 67, 793-805.
680   WOLFF, E. W., CHAPPELLAZ, J., BLUNIER, T., RASMUSSEN, S. O. & SVENSSON, A. 2010. Millennial-scale variability
681   during the last glacial: the ice core record. *Quaternary Sci. Rev.,* 29, 2828-2838.
682   XUE, J., ZHONG, W., ZHAO, Y. & PENG, X. 2008. Holocene abrupt climate shifts and mid-Holocene drought intervals
683   recorded in Barkol Lake of Northern Xinjiang of China. *Chinese Geogr. Sci.,* 18, 54-61.
684   YANG, S., ODAH, H. & SHAW, J. 2000. Variations in the geomagnetic dipole moment over the last 12 000 years.
685   *Geophys. J. Int.,* 140, 158-162.
686   YIOU, F., RAISBECK, G. M., BAUMGARTNER, S., BEER, J., HAMMER, C., JOHNSEN, S., JOUZEL, J., KUBIK, P. W.,
687   LESTRINGUEZ, J., STIÉVENARD, M., SUTER, M. & YIOU, P. 1997. Beryllium 10 in the Greenland Ice Core
688   Project ice core at Summit, Greenland. *J. Geophys. Res.,* 102, 26783-26794.
689   YOUSEF, S. M. 2000. The solar Wolf-Gleissberg cycle and its influence on the Earth. *International Conference for*
690   *Environmental Hazard.* Cairo: Cairo University.

691